Published in final edited form as:
Invest Ophthalmol Vis Sci. 2009 June ; 50(6): 2989–2993. doi:10.1167/iovs.08-2542.

In vivo imaging of the Mouse Model of X-Linked Juvenile Retinoschisis Using Fourier Domain Optical Coherence Tomography

Jing Xu[1], **Laurie L. Molday**[2], **Robert S. Molday**[2], and **Marinko V. Sarunic**[1]

1*School of Engineering Science, Simon Fraser University, Burnaby, BC V5A 1S6, Canada.*

2*Department of Biochemistry & Molecular Biology, Centre for Macular Research, University of British Columbia, Vancouver, B.C. V6T 1Z3, Canada.*

Abstract

Purpose—The purpose of this study is to investigate Fourier Domain Optical Coherence Tomography (FD OCT) as a non-invasive tool for retinal imaging in the *Rs1h* knockout mouse (model for X-linked Juvenile Retinoschisis).

Methods—A prototype spectrometer based FD OCT system was used in combination with a custom optical beam-scanning platform. Images of the retinas from wild type and *Rs1h* knockout mice were acquired non-invasively using FD OCT with the specimen anesthetized. At the completion of the non-invasive FD OCT imaging, invasive retinal cross sectional images (histology) were acquired from a nearby region for comparison to the FD OCT images.

Results—The retinal layers could be identified in the FD OCT images, permitting delineation and thickness measurement of the outer nuclear layer (ONL). During FD OCT *in vivo* imaging of the *Rs1h* knockout mouse, holes were observed in the inner nuclear layer (INL) and retinal cell disorganization was observed as a change in the backscattering intensity profile. Comparison of the ONL measurements acquired non-invasively using FD OCT to measurements taken using histology at nearby locations showed a degeneration of roughly thirty percent of the ONL by the age of two months in *Rs1h* knockout mice relative to wild type.

Conclusions—FD OCT has been demonstrated for non-invasive imaging of retinal degeneration and observation of retinal holes in *Rs1h* knockout mice.

Introduction

Significant inroads have been made by Fourier Domain Optical Coherence Tomography (FD OCT) into human retinal imaging.[1–8] As the FD OCT imaging modality is gaining wider acceptance for its diagnostic utility, the investigation of FD OCT as a tool for basic visual science with animal models of retinal degeneration is also generating increasing interest. In contrast to human clinical imaging where only non-invasive imaging modalities can be used, research involving animal models can use invasive histology on enucleated eyes, permitting confocal imaging of immunological stained sections to enhance contrast of retinal features. Non-invasive imaging with FD OCT has the distinct advantage of facilitating longitudinal studies on the time course of diseases, and has the potential to accelerate basic medical research by significantly reducing the number of animals required. Furthermore, non-invasive imaging

Corresponding Author: Marinko V. Sarunic, Simon Fraser University, 8888 University Drive, Burnaby, BC V5A 1S6, Tel: (778) 782 7654, Fax: (778) 782 4951.

with FD-OCT has the ability to identify abnormal structural morphology *in vivo*, removing concerns of potential tissue processing artifacts introduced by histology.

Attempts to investigate retinal degeneration in mice with early time domain OCT systems were hampered due to low resolution and slow image acquisition.[9–11] Investigation of retinal degeneration with FD OCT in rodents is at an early stage, and to date only wild type (WT) specimen and simple models of retinal degeneration have been imaged.[12–14] Two techniques of focusing the light on the rodent retina have been investigated. In one approach[13] a collimated beam was used, relying on the refractive elements of the mouse eye to focus the beam to a spot on the retina. In another approach [12, 14] a focused beam was used in conjunction with a contact lens to cancel out the refraction by the cornea. Irrespective of the technique used, the retinal layers could be identified based on their relative scattering intensity, similar to human retinal imaging. An investigation of FD OCT for a time course study of retinal degeneration in the *rd1* mouse was presented in [14] using a pulsed femtosecond titanium:sapphire laser providing 110nm of bandwidth at an 800nm center. Degeneration was quantified by comparing the ratio of the thickness of the outer retina (including the layers from the outer plexiform layer (OPL) to the outer segment (OS) of the photoreceptor layer) to the thickness of the whole retina (including the layers from the nerve fiber layer (NFL) to the OS).

In this report we build on the existing literature studying FD OCT as a non-invasive imaging modality to study retinal degeneration in mice *in vivo*. The mouse model for X-linked Juvenile Retinoschisis (RS), a form of genetic retinal degeneration in males, was investigated in this FD OCT research application. These knockout mice are deficient in the *Rs1h* gene, the ortholog to the *RS1* gene in humans, and have been shown through histology to be characterized by holes in the inner nuclear layer (INL),[15] disorganization of the retinal cell layers, and slow progressive degeneration of the photoreceptors. We present a comparison of non-invasive retinal imaging in *Rs1h* knockout (KO) and wild type mice acquired with the FD OCT to invasive histological sections. Qualitatively, disorganization of the retinal morphology associated with *Rs1h* knockout mouse was observed with FDOCT, as well as holes in the INL characteristic of retinoschisis. The application of FD OCT to provide quantitative measurements was also investigated. The metric used to quantify the amount of retinal degeneration was the thickness of the Outer Nuclear Layer (ONL) which thins with increasing age in *Rs1h* mice. Two dimensional maps of the ONL thickness were extracted from the FD OCT volume data acquired on wild type and *Rs1h* knockout mice. From the standpoint of evaluating a research tool, the FD OCT system used in this study utilized a cost-effective and portable continuous superluminescent diode (SLED) light source, nominally one tenth the cost of an exotic femtosecond laser, and a custom sample arm constructed from bulk achromatic lenses.

Methods

FD OCT

A prototype FD OCT system was constructed for mouse retinal imaging. The standard interferometer topology used in this report, presented in Figure 1, consisted of a source, fiber coupler, and custom spectrometer based detection. The SLED source (Superlum, Moscow, Russia) had a central wavelength of 826nm and a spectral bandwidth full width half maximum (FWHM) of 72nm. The corresponding transform limited axial resolution was nominally 4 μm in tissue. During animal imaging, the optical power output from the source was reduced to 770μW, the ANSI limit for maximum exposure of the retina to continuous light at this wavelength.[16] The interferometer was constructed from a 2×2 fiber coupler (AC Photonics, Santa Clara, USA) with an 80/20 splitting ratio. This configuration was used to provide 20% of the source light to the sample arm, but in the reverse direction, 80% of the collected light was directed to the detector in order to optimize the optical signal. The reference arm consisted

simply of a collimating lens, attenuator, and mirror. Dispersion was corrected purely through numerical techniques,[4] and no additional optics were included in the reference arm. The sample arm consisted of a collimating lens followed by a pair of galvanometer mounted mirrors for raster scanning control of the beam. The beam expander and objective lenses following the scanning mirrors, as indicated in Figure 1, were constructed from anti-reflection coated achromatic lenses. The calculated spot size given the optical configuration was nominally 13 μm with a depth of focus of 350 μm, designed to provide high resolution lateral images, while spanning the full retinal thickness. The sample arm optics were mounted on a slit-lamp biomicroscope stage for positioning of the beam relative to the mouse eye.

The high speed spectrometer used was a custom design constructed using a 1200 l/mm transmission diffraction grating. The detector was a 1024 element high speed Gigabit Ethernet (GigE) camera from Dalsa (Waterloo, Canada), with 10 μm square pixels. The camera could operate at a maximum line rate of 68kHz, but was typically reduced to 20kHz for imaging. Data acquisition was performed using custom software written in C++ for rapid frame grabbing, processing, and display of two dimensional images. Processing performed in real time included re-sampling of the interferometric data from linearly sampled in wavelength space to linear sampling in wavenumber space, fast Fourier transform (FFT), as well as image contrast and brightness. Dispersion compensation was also performed by the software up to the third term, but was limited to real time display of nominally 30 frames per second under imaging conditions of 512 lines per frame.

FD OCT Mouse Imaging

Although the FD OCT imaging is non-invasive, in order to keep the mice still during imaging they were anesthetized using an intraperitoneal injection of ketamine and xylazine mixture (0.1ml per 10 g body weight). After anesthetization, the mouse was placed gently on a heating pad to maintain warmth, and simple manual manipulation was used to rest the head of the mouse in an orientation where the angle of the eye was properly coupled to the optical beam. The pupils were dilated using a topical solution (atropine sulphate 1%). Refraction of light at the cornea was cancelled by placing a flat coverslip generously coated with a generic artificial tear gel over the eye. Alignment of the optical system to the mouse retina required several minutes, and was followed by rapid acquisition of data, requiring nominally 5 seconds per volume. During imaging, the software displayed the FD OCT B-scans at ~30 frames per second. Registration of the location of the B-scan within the two dimensional surface of the retina was performed by switching the display mode to a higher speed (60kHz line rate), low sampling density area scan, representing a reconstructed fundus type image. All mouse handling adhered to the ARVO Statement for the Use of Animals in Ophthalmic and Vision Research, and were performed under protocols compliant to the Canadian Council on Animal Care with the approval of the University Animal Care Committee at SFU.

The ONL thickness measurements were extracted by post processing saved data. A fundus type image of the mouse retina was reconstructed using the FD-OCT volumetric data,[7] and used to register the location of the ONL thickness measurement 400 micrometers from the optic nerve head where the retinal layers were of nominally constant cross section. The ONL boundaries were delineated by manually placing points at the boundary between layers, and fitting a low order polynomial to the points using mathematical software package MatLab (MathWorks, Natick, MA, USA). The ONL thickness was subsequently measured along a line in the image, and was calculated perpendicular to the curvature of the retina using Snell's law calculations to account for refractive index changes.[17, 18] The estimated average refractive index of the retina was $n_{retina} = 1.38$. The recorded ONL thickness for a given eye was calculated as the mean of three adjacent depth profile frames to average out human error in delineation of the ONL boundaries. Automated computer segmentation of the depth profiles

using advanced image processing algorithms is under development to complement the FD-OCT image acquisition and reduce inter-observer variation. Following the non-invasive FD OCT measurement, the mice were euthanized and the eyes were enucleated for histology.

Histology

Immediately following FD OCT measurements (hours), the mice were sacrificed and the eyes were enucleated and fixed in 4% paraformaldehyde / in 0.1M phosphate buffer, pH 7.2 for 15 hours. After fixation, the samples were washed and frozen in O.C.T. compound, cut into 12μm sections and stained with DAPI nuclear stain. The retina sections were visualized with under a Zeiss Axioplan fluorescence microscope and the ONL thickness was measured by counting the number of nuclei at five locations in the DAPI stained histological sections.

Results

Correlation of FD OCT depth profiles with histological sections

Cross sectional depth profiles in FD OCT consist of alternating bright and dark regions, corresponding to the backscattering intensity of the various retinal layers. The retinal layers can be identified in the FD OCT images through comparison with a histological section as shown in Figure 2 (a, b). The thickness of the outer nuclear layer (ONL) was measured as the distance of the dark band between the bright lines constituting the outer plexiform layer (OPL) and the inner segment (IS) of the photoreceptor layer. In order to measure the thickness of the ONL, each FD OCT image was first manually segmented by selecting points on each curved boundary and fitting them to a low order polynomial, as described in the Methods section. In Figure 2 (b), the OPL/ONL boundary is indicated by the green line fit to the manually selected points represented by the circles. The ONL/IS boundary was similarly delineated, and is represented in yellow.

Retinal Structure in the Rs1h knockout mice

In the FD OCT images, irregularities in the retinal layer structure of the *Rs1h* knockout mouse were observed relative to the wild type. A sample FD OCT image of a *Rs1h* KO mouse is shown adjacent to a histological section in Figure 2 (c, d). The OPL layer and the IS/OS photoreceptor layers appear thicker in the FD OCT image due to poorly defined ONL boundaries. In the DAPI stained histological image, the OPL between the ONL and INL is not well resolved. Characteristic to retinoschisis, holes or cavities were also observed in the INL layers in the FD OCT images and also in the histological sections.

ONL Thickness Measurements with FD OCT and histology

For this study, we compared measurements of the ONL thickness in *Rs1h* knockout (KO) mice to that of their wild type counterparts. The ONL thickness was measured in both eyes of each specimen used. The control group consisted of 6 wildtype mice for the FD OCT measurement, corresponding to a sample size of $n = 12$ eyes. The control group for the DAPI stained histology control group consisted of five specimens, corresponding to a sample size n=10. Two mice were used for each age group of *Rs1h* KO investigated, making a sample size of $n_{RS1hXmo}$=4 eyes (*X* represents the age of the specimen in months). Three different ages of *Rs1h* KO mice were used in this study: two months, ten months, and fifteen months. The reported values of ONL thickness represent the average and standard deviation of the n measurements from each group.

Examples of the fundus reconstruction and depth profile images acquired with the FD-OCT are presented alongside DAPI stained histology in Figure 3. The fundus image represents a volumetric data set; a FD-OCT depth scan of information is contained in each horizontal line.

The numerical results of the ONL thickness measurements comparing FD-OCT to DAPI stained histology are summarized in Table 1. The ratio was calculated using the average ONL thickness measurement from each *Rs1h* KO group and dividing it by that of the corresponding control group. Standard error propagation was used based on the standard deviation of the group averages. The measured differences in ONL thickness between *Rs1h* KO mice of neighboring age groups in the time course study was statistically significant (p value < 0.01, by ANOVA).

Discussion

Non-invasive imaging of the mouse retina can be a powerful tool for characterization of retinal degeneration. Imaging mice with the FD OCT system poses a different set of challenges than human retinal imaging. The FD OCT configuration for imaging humans typically uses a collimated beam of light incident on the eye, relying on the refractive elements of the cornea and lens to focus the beam on the retina. In our investigation, we found it preferable to cancel out the refraction at the cornea with a contact lens and perform FD OCT imaging of the mouse eye using a converging beam.[12]

Comparison of the *Rs1h* knockout mouse retina images in Figure 3 to the wild type counterparts indicates a marked difference in the retinal layer structure. Most noticeably, the OPL and IS/OS layers were not well defined in the FD OCT images of the *Rs1h* knockout mouse retina, and appeared as broader regions of high scattering intensity. This is consistent with earlier reports using histology where the disruption of the cell layer architecture was notable in the OPL between the ONL and INL.[15]

In addition the disorganization of the retinal layers in the *Rs1h* knockout mice, superficial holes in the INL layer were also observed in Figure 2 (d) as dark regions with no backscattered light signal. Since shadows of lower scattering intensity were not cast below the holes in the INL, we can conclude that the gaps must be full of a clear non-scattering fluid. Similar results of holes in the INL had been previously observed in histological samples of this strain of mice, [15] but due to the physical manipulation of the retinal samples in histological preparation, it was not clear if the gaps were due to delamination of the cell-to-cell contacts in the INL or if the holes were present in the normal physiology. Due to the non-invasive nature of FD OCT imaging, we can conclusively confirm that the retinal holes in the ONL were not artifacts of histology. The holes observed in the FD OCT images of the *Rs1h* knockout mouse can also be compared with the observation of schisis cavities in the FD OCT images of humans with X-linked Juvenile Retinoschisis.[19–21] These images demonstrate that FD OCT has the potential to be used to non-invasively monitor the size and number of the retinal holes, and provide feedback on the progress of retinal therapy without destroying the specimen.

Quantitative measurements of retinal degeneration were extracted from the data presented in Figure 3 to monitor the relative thickness of the ONL in the *Rs1h* knockout mice relative to wild type mice. The averaged ONL thickness measurement of the *Rs1h* KO mice obtained with the FD OCT and with histology is summarized in Table 1. The average thickness of the ONL in wild type mice (independent of age) measured with FD OCT was μ_{WT} = 46μm, SD= 2μm (n = 12). The standard deviation is less than the axial resolution of the system (~4μm in tissue) and indicates a reasonable correlation of thickness measurements across all of the animals and in both eyes. The average ONL thickness measurement in wild type mice obtained by counting nuclei in the DAPI stained histology was μ_{WT} =11.4 nuclei, SD = 1 nuclei (n = *10*), indicating an uncertainty of 9% in the wild type mice.

The amount of retinal degeneration in the *RS1h* knockout mice relative to their wild type counterparts is also summarized in Table 1. For two month old mice, the FD OCT

measurements indicated that the ONL in *Rs1h* knockout mice had degenerated to μ=69%, SD 3% (*n=4*) of the wild type ONL thickness. This measurement was statistically within experimental error of the same measurement made through histology. Further degeneration of the ONL was observed in the 10 month old *Rs1h* KO mice; with the FD OCT, the measured ratio ONL_{RS1h}/ONL_{WT} was μ=59%, SD 3% (*n=4*). This measurement also agreed with the DAPI stained histology measurements within experimental error. The measured ratio of ONL thickness in the 15 month old *Rs1h* KO mice relative to the wild type was μ=36%, SD 2% (*n=4*). However, due to the advanced degeneration of the ONL and severe disorganization of the retinal layers observed (Figure 3 g, h), delineation of the ONL thickness by FD OCT or DAPI stained histology was nontrivial.

The thickness of the ONL in *Rs1h* KO mice was measured for two additional age groups, five months and fourteen months. The histology measurements for these mice followed the trend observed in the other groups. The FD OCT measurements were used to graph the change in ONL thickness across the age groups; the data is presented in Figure 4 (a). The graph suggests that the retinal degeneration in *Rs1h* KO mice is gradual between the ages of two months and nominally one year, at which point the rate of degeneration appears to increase.

The disorganization of the retinal layers in the *Rs1h* knockout mice made it difficult to establish definite boundaries of the ONL, which added to the measurement uncertainty of this study. These issues are present in both the histological and FD OCT measurements; however the ability to average over multiple images using FD OCT presents a definite advantage of the non-invasive technique. An option to improve the repeatability in the ONL thickness measurement would be to use automated segmentation software in order to eliminate human error and inter-observer variation in the delineation of the ONL boundaries. With automated segmentation of the layers, the ONL thickness measurement with FD OCT can also be extended to a large area of the retina by processing the entire volume of data contained in the reconstructed fundus-type images shown in Figure 3 (a, b). Two dimensional thickness maps of the ONL in a two month old wild type mouse and an age matched *Rsh1* KO mouse were processed and displayed in Figure 4 (b, c). Due to the manual labor required to segment the depth profiles in an entire volume, only every tenth elevation frame was extracted from the data to generate the thickness maps. In agreement with the results summarized in Table 1, the thickness maps in Figure 4 (b, c) indicate that the ONL was thinner in the *Rs1h* knockout mouse than in the wild type mouse. Automated segmentation of the retinal layers would benefit this application by providing higher spatial detail in the two dimensional thickness maps by permitting processing of each acquired frame.

Conclusion

Non-invasive FD OCT imaging of the sub-surface retinal layers has been used to measure the thickness of the ONL in mice with retinal degeneration. In this study, we concentrated on the use of cost-effective and portable equipment for the FD OCT system. We compared the thickness measurements of the ONL in wild type mice to thinning of the ONL in *Rs1h* knockout mice, the model for X-linked Juvenile Retinoschisis. Comparison of the non-invasive FD OCT measurements to histology demonstrated a strong correlation, and the measurement results matched within experimental uncertainty. At two months of age, the ONL layers in the *Rs1h* knockout mice had thinned down to nominally seventy percent of the wild type thickness. By an age of fifteen month, the thickness of the ONL layer in Rs1H KO mice was nominally a third of the wild type. FD OCT also provided non-invasive images of the general disorganization of the retinal cell layers in the *Rs1h* knockout mice, and was also able to image holes in the INL associated with the deficiency of retinoschisin.

Grant Acknowledgements

We acknowledge support from NSERC Discovery Grant (31-11498) and MSFHR Career Investigator Award to MVS and NEI grant (EY 02422) and Foundation Fighting Blindness Grant to RSM.

References

1. Huang D, Swanson EA, Lin CP, Schuman JS, Stinson WG, Chang W, Hee MR, Flotte T, Gregory K, Puliafito CA, Fujimoto JG. Optical Coherence Tomography. Science 1991;254:1178–1181. [PubMed: 1957169]
2. Fercher AF, Hitzenberger CK, Kamp G, Elzaiat SY. Measurement of Intraocular Distances by Backscattering Spectral Interferometry. Optics Communications 1995;117(1–2):43–48.
3. Cense B, Nassif N, Chen TC, Pierce MC, Yun SH, Park BH, Bouma BE, Tearney GJ, de Boer JF. Ultrahigh-resolution high-speed retinal imaging using spectral-domain optical coherence tomography. Optics Express 2004;12(11):2435–2447. [PubMed: 19475080]
4. Wojtkowski M, Srinivasan VJ, Ko TH, Fujimoto JG, Kowalczyk A, Duker JS. Ultrahigh-resolution, high-speed, Fourier domain optical coherence tomography and methods for dispersion compensation. Optics Express 2004;12(11):2404–2422. [PubMed: 19475077]
5. Leitgeb RA, Drexler W, Unterhuber A, Hermann B, Bajraszewski T, Le T, Stingl A, Fercher AF. Ultrahigh resolution Fourier domain optical coherence tomography. Optics Express 2004;12(10): 2156–2165. [PubMed: 19475051]
6. Bower, BA.; Zhao, M.; Zawadzki, RJ.; Sarunic, MV.; Izatt, JA. Coherence Domain Optical Methods and Optical Coherence Tomography in Biomedicine IX. San Jose, CA: SPIE; 2005. Rapid volumetric imaging of the human retina in vivo using a low-cost, Fourier domain optical coherence tomography system.
7. Jiao SL, Knighton R, Huang XR, Gregori G, Puliafito CA. Simultaneous acquisition of sectional and fundus ophthalmic images with spectral-domain optical coherence tomography. Optics Express 2005;13(2):444–452. [PubMed: 19488371]
8. Drexler W, Fujimoto JG. State-of-the-art retinal optical coherence tomography. Prog Retin Eye Res 2008;27(1):45–88. [PubMed: 18036865]
9. Li QH, Timmers AM, Hunter K, Gonzalez-Pola C, Lewin AS, Reitze DH, Hauswirth WW. Noninvasive imaging by optical coherence tomography to monitor retinal degeneration in the mouse. Investigative Ophthalmology & Visual Science 2001;42(12):2981–2989. [PubMed: 11687546]
10. Kocaoglu OP, Uhlhorn SR, Hernandez E, Juarez RA, Will R, Parel JM, Manns F. Simultaneous fundus imaging and optical coherence tomography of the mouse retina. Invest Ophthalmol Vis Sci 2007;48(3):1283–1289. [PubMed: 17325174]
11. Horio N, Kachi S, Hori K, Okamoto Y, Yamamoto E, Terasaki H, Miyake Y. Progressive change of optical coherence tomography scans in retinal degeneration slow mice. Archives of Ophthalmology 2001;119(9):1329–1332. [PubMed: 11545639]
12. Srinivasan VJ, Ko TH, Wojtkowski M, Carvalho M, Clermont A, Bursell SE, Song QH, Lem J, Duker JS, Schuman JS, Fujimoto JG. Noninvasive volumetric imaging and morphometry of the rodent retina with high-speed, ultrahigh-resolution optical coherence tomography. Invest Ophthalmol Vis Sci 2006;47(12):5522–5528. [PubMed: 17122144]
13. Ruggeri M, Wehbe H, Jiao S, Gregori G, Jockovich ME, Hackam A, Duan Y, Puliafito CA. In vivo three-dimensional high-resolution imaging of rodent retina with spectral-domain optical coherence tomography. Invest Ophthalmol Vis Sci 2007;48(4):1808–1814. [PubMed: 17389515]
14. Kim KH, Puoris'haag M, Maguluri GN, Umino Y, Cusato K, Barlow RB, de Boer JF. Monitoring mouse retinal degeneration with high-resolution spectral-domain optical coherence tomography. J Vis 2008;8(1):17, 1–11. [PubMed: 18318620]
15. Weber BH, Schrewe H, Molday LL, Gehrig A, White KL, Seeliger MW, Jaissle GB, Friedburg C, Tamm E, Molday RS. Inactivation of the murine X-linked juvenile retinoschisis gene, Rs1h, suggests a role of retinoschisin in retinal cell layer organization and synaptic structure. Proc Natl Acad Sci U S A 2002;99(9):6222–6227. [PubMed: 11983912]
16. ANSI. American National Standard for Safe Use of Lasers, ANSI Z 136.1-1993. Orlando, Fla: The Laser Institute of America; 1993. p. 37-43.

17. Sarunic MV, Asrani S, Izatt JA. Imaging the ocular anterior segment with real-time, full-range Fourier-domain optical coherence tomography. Arch Ophthalmol 2008;126(4):537–542. [PubMed: 18413525]

18. Zawadzki, RJ.; Leisser, C.; Leitgeb, R.; Pircher, M.; Fercher, AF. SPIE Biomedical Optics. San Jose, CA: 2003. 3D ophthalmic OCT with a refraction correction algorithm.

19. Apushkin MA, Fishman GA. Use of dorzolamide for patients with X-linked retinoschisis. Retina 2006;26(7):741–745. [PubMed: 16963845]

20. Apushkin MA, Fishman GA, Janowicz MJ. Correlation of optical coherence tomography findings with visual acuity and macular lesions in patients with X-linked retinoschisis. Ophthalmology 2005;112(3):495–501. [PubMed: 15745780]

21. Gerth C, Zawadzki RJ, Werner JS, Heon E. Retinal morphological changes of patients with X-linked retinoschisis evaluated by Fourier-domain optical coherence tomography. Arch Ophthalmol 2008;126(6):807–811. [PubMed: 18541843]

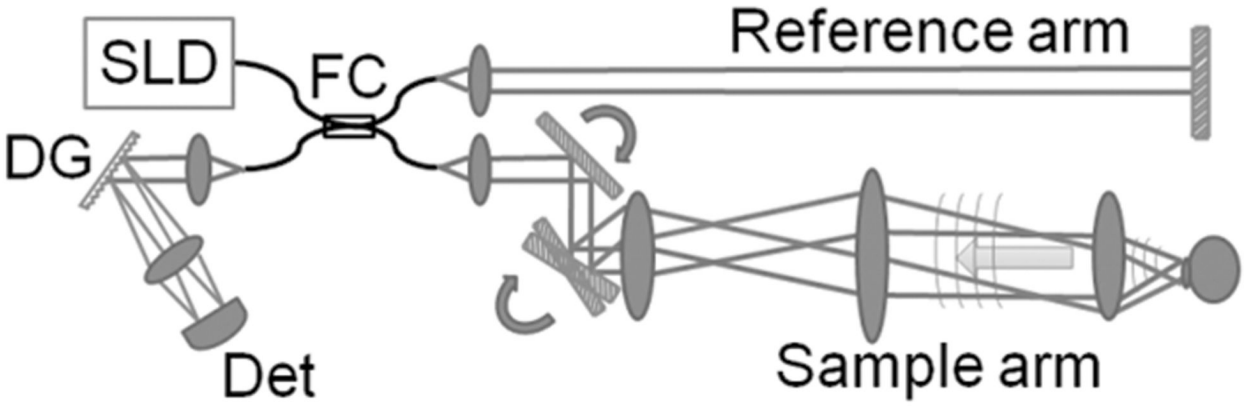

Figure 1.
Schematic diagram of the FD OCT interferometric setup used to image the mouse retina.

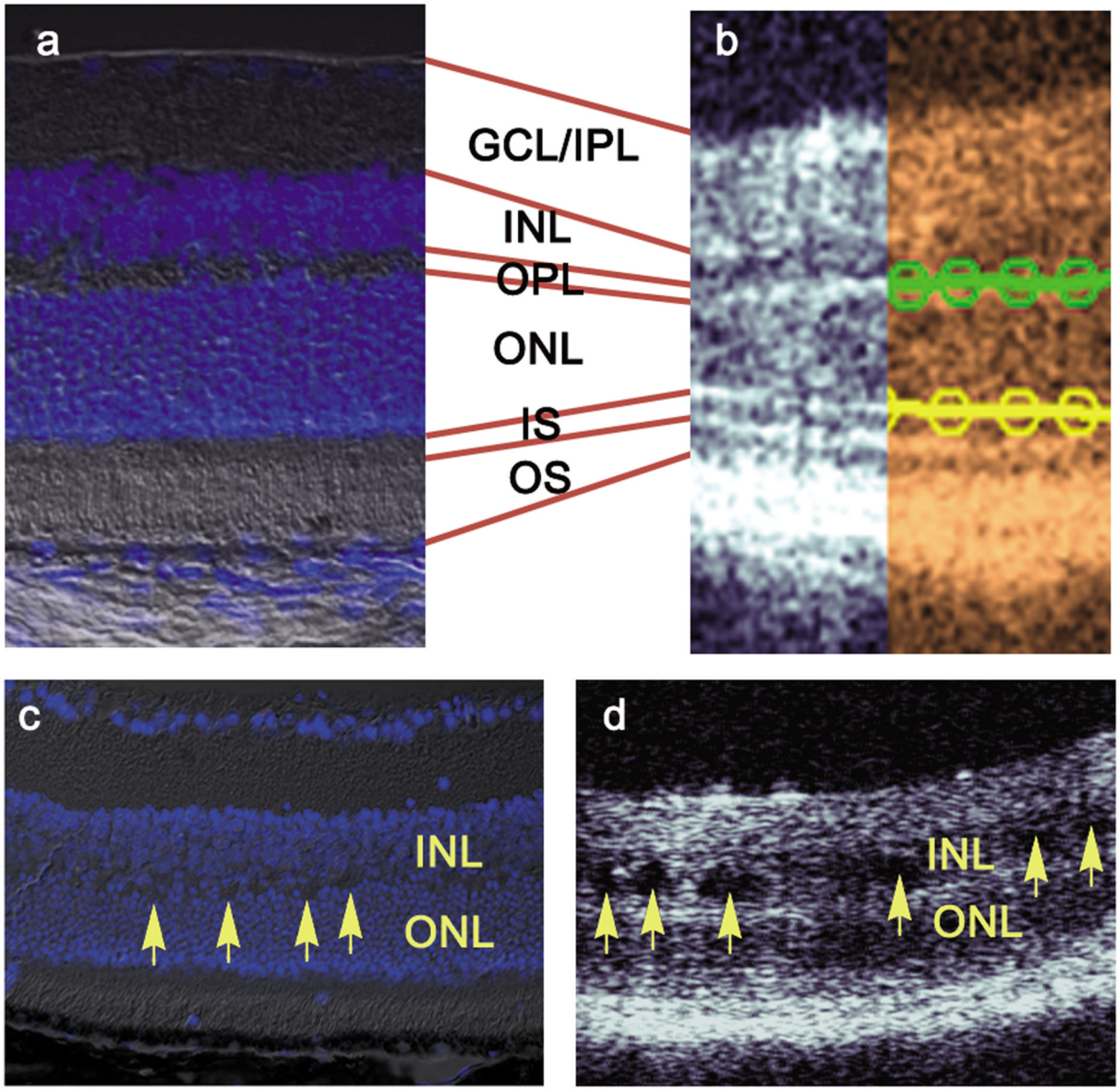

Figure 2.

Comparison of the wild type mouse retinal layers observed in (a) DAPI stained histological section merged with DIC to (b) non-invasive FD OCT. The retinal layers were segmented manually and a fit to a fourth order polynomial which was subsequently used for the thickness measurement. Arrows point to holes observed in the inner nuclear layer (INL) of (c) DAPI stained histology and (d) FD OCT image of the retina of a two month old *Rs1h* knockout mouse. GCL, ganglion cell layer; IPL, inner plexiform layer; OPL, outer plexiform layer, ONL, outer nuclear layer; IS, inner segment; OS, outer segment.

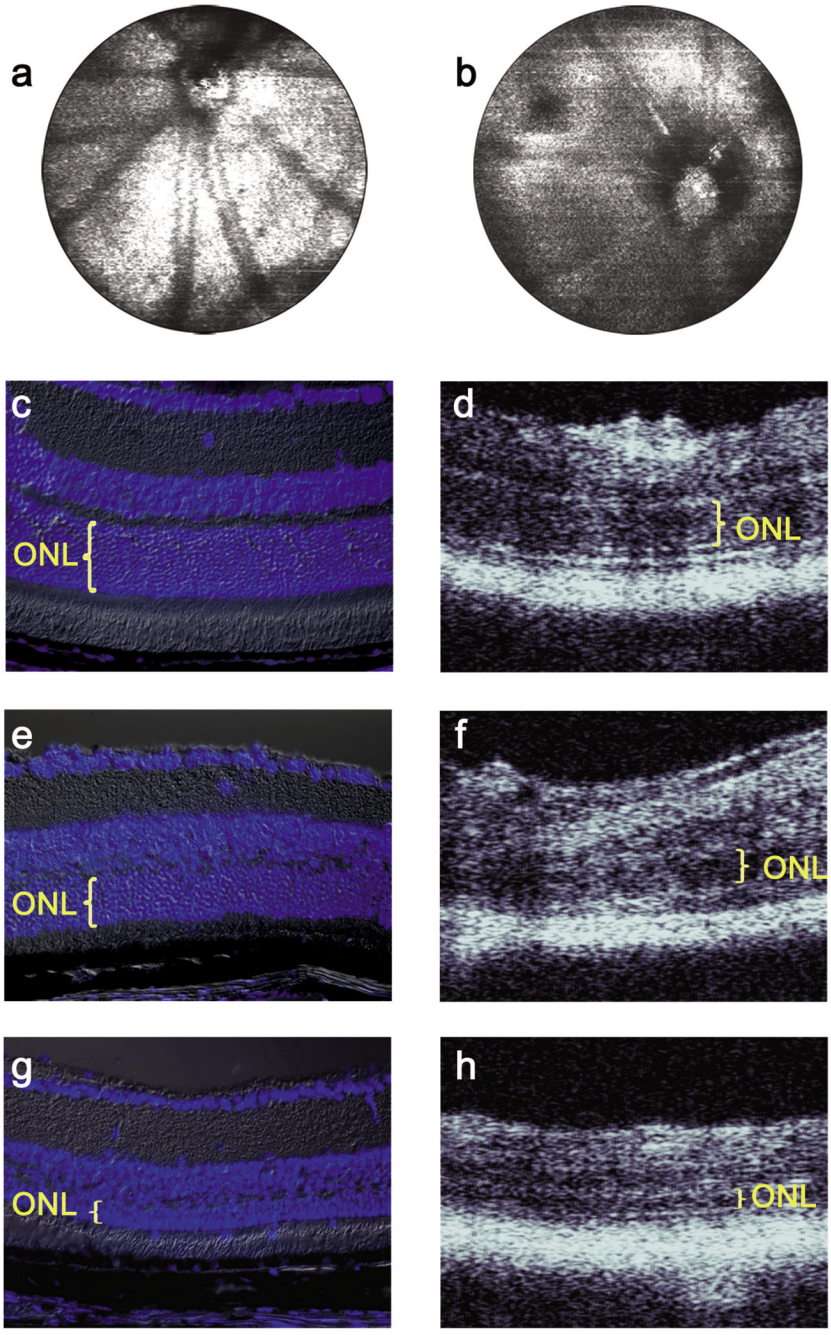

Figure 3.
Fundus-type images reconstructed from FD OCT data acquired from (a) WT and (b) *Rs1h* KO mice. DAPI stained histology and FD-OCT images from the same mice are shown for (c, d) 2 month old WT, (e, f) 2 month old *Rs1h* KO, (g, h) 15 month old *Rs1h* KO.

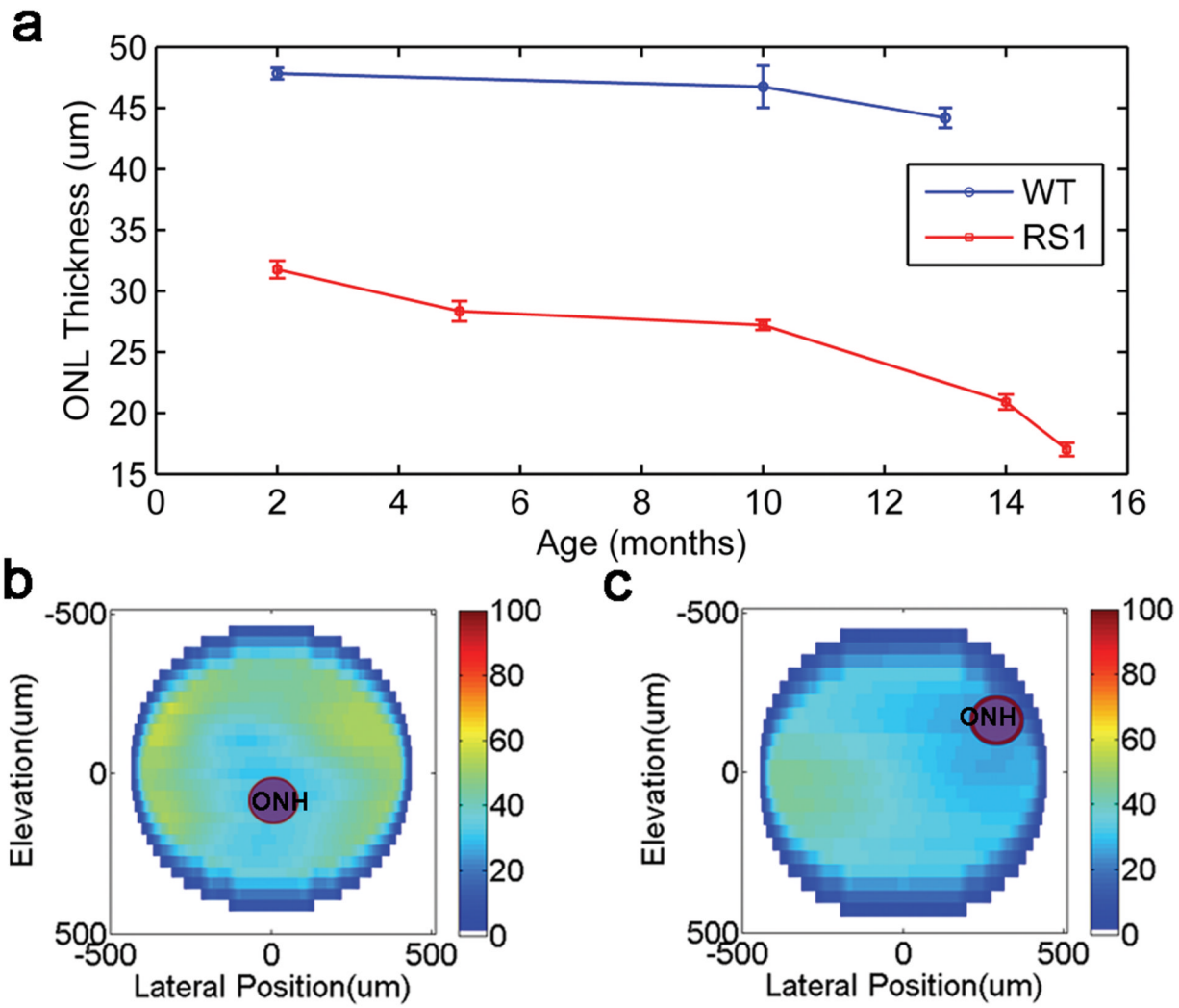

Figure 4.
(a) ONL thickness of wild type and *Rs1h* KO mice measured with FD OCT for different age groups. Two dimensional map of the ONL thickness for (b) wild type and (c) *Rs1h* knockout mouse at two months of age.

Table 1

ONL thickness measurements from *Rs1h* KO mice using FD OCT and DAPI stained histology. The ratio was calculated using the ONL thickness of the control group. Nuc., Number of nuclei counted from histology.

	Measured Thickness				Ratio			
	OCT		Histology		*Rs1h*/WT			
month	μm	SD	Nuc.	SD	OCT	SD	Nuc.	SD
2	31.8	0.7	7.6	0.4	0.69	0.03	0.67	0.07
10	27.2	0.4	6.4	0.6	0.59	0.03	0.56	0.07
15	17.0	0.5	3.1	0.5	0.37	0.02	0.28	0.05